Geophys. J. R. astr. Soc. (1984) 77, 461–482

Admittance for a convection in a layered spherical shell

B. Lago and M. Rabinowicz *Centre National d'Etudes Spatiales, Groupe de Recherche de Geodesie Spatiale, 18, Avenue Edouard Belin, 31055 Toulouse cedex, France*

Received 1983 August 8; in original form 1983 January 7

Summary. A formalism based on an analytical approximation for convection in a layered spherical shell leads to the computation of the Green kernels for topography and gravity, and to the admittance of gravity over topography for the harmonics of the Earth. We study the role of increasing viscosity with depth, of two layers of convection, and of the coupling with lithospheric plates. It is found that a planet with constant viscosity will have positive values for the admittance for all wavenumbers. However, when a step of viscosity between the lower and upper mantle is assumed, negative values for the first harmonics are achieved. This result explains some long-wave observations and provides evidence for an increase of viscosity in the lower mantle.

1 Introduction

Transfer functions of gravity or geoid over topography have been used by many authors in order to understand the response of the lithosphere to loads (Watts 1978) or more recently to localized heat sources in the asthenosphere (Sandwell 1982) and then to discuss the relative importance of different compensation mechanisms within the lithosphere due to a local Airy or Pratt isostasy, to regional lithospheric deflection or to the thermal evolution of the lithosphere.

McKenzie (1977) and Parsons & Daly (1984) extend these studies to larger wavelengths, which are thought to be associated with convection in the upper mantle. They prove using both numerical and analytical models that the admittance for small-scale aspect ratio (~ 700 km of horizontal extent) convective cells in a constant viscosity upper mantle must be positive and close to 0.3, implying that gravity anomalies are respectively positive over the ascending limb of a convective cell and negative over the descending one. Such theoretical results are found to be in good agreement with some observed data. For example, the positive correlation between $5^\circ \times 5^\circ$ mean gravity and residual depth anomalies over the

Hawaian swell has been explained by an upward warm flow within the mantle maintaining both the swell and the observed positive long-wavelength gravity anomalies (Watts 1976); a correlation between geoid height and bathymetry in the Pacific and Indian Oceans has been interpreted in the same way (McKenzie *et al.* 1980).

Nevertheless one can question if these results can be extended to larger wavelength or convective modes. As emphasized by Runcorn (1972) and Kaula (1972) gravity anomalies over subduction zones deduced from satellite models present large positive values over the subduction zone, which are believed to be downwelling regions of the convective circulation, implying that over these regions the sign of the admittance should be negative.

A careful modelling of the convective flow driven by the subducting slab acting as a heat sink shows that the convective cells driven by the sinking slab in the upper mantle have a large aspect ratio, at least equal to 5, and thus have a horizontal extent of at least 3000 km (Rabinowicz, Lago & Froidevaux 1980; Nataf *et al.* 1981). It is shown that the shape of the gravity signal associated with these cells can be quite different from that of small aspect ratio cells (Rabinowicz, Lago & Souriau 1983). We showed that the negative admittance values necessary to explain the observed gravity signal landward of the subduction zones can be achieved if some dynamical support is given by convection in the lower mantle. These considerations lead us to estimate admittance in a multilayered spherical shell with a possible variation of viscosity versus depth, and to calculate the modal response of the plastic flow to a harmonic component of the temperature excitation, as well as the associated surface deformation and gravity kernels. General characteristics of the formalism are given in Section 3 with some complements in Appendices A and B, while a set of results are shown and commented on in Section 3. Certain geophysical implications are discussed in Sections 4 and 5.

2 The formalism

The proposed formalism generalizes McKenzie's (1977) approach and considers Green function and height and gravity kernels as in Parsons & Daly (1984). A relatively similar formalism can also be found in Ricard, Fleitout & Froidevaux (1984).

Classical equations useful for our formalism can be found for example in Chandrasekar (1961, chaper VI).

The very large value of the Prandtl number in the Earth's mantle allows us to ignore the term in 'd/dt' and, as the Boussinesq approximation is considered, perturbations to reference profiles of the pressure (δp) and temperature T allows us to write the equation of motion in Cartesian coordinates (x_1, x_2, x_3) in the following form:

$$-\frac{\partial}{\partial x_i}\left(\frac{\partial P}{\rho}+\delta V\right)+\alpha\frac{g(r)}{r}Tx_i+\nu\nabla^2 U_i=0, \tag{1}$$

where r is the distance to the origin, U_i the velocity components, ρ the density, δV the disturbing gravity potential, α the coefficient of volume expansion, $g(r)$ the gravity and ν the kinematic viscosity.

To this equation is added the equation of continuity (a non-compressibility condition is assumed):

$$\sum_{i=1}^{3}\frac{\partial U_i}{\partial x_i}=0. \tag{2}$$

Taking the curl of (1) allows us to eliminate the term in grad $\delta P/\rho + \delta V$; taking the curl^2 of (1) allows us to write:

$$\nu\nabla^4 U_i = \sum_{j=1}^{3} \frac{\partial}{\partial x_j} \frac{\alpha g(r)}{r} \left(x_j \frac{\partial T}{\partial x_i} - x_i \frac{\partial T}{\partial x_j} \right) \tag{3}$$

No equation concerning T will be written; we will consider a component of the thermal field T of the form $\tau(r)\, Y_l^m(\theta, \phi)$ where r, θ, ϕ are the spherical coordinates, Y_l^m a spherical harmonic and $\tau(r)$ a test function.

This given component of the thermal field generates a poloidal component of the flow; a function $W(r)$ is associated with this poloidal component, such that:

$$\sum_{i=1}^{3} x_i U_i = r U_r = W(r)\, Y_l^m(\theta, \phi).$$

This gives for the components of the velocity in the spherical tangential frame:

$$\left.\begin{aligned} U_r &= \frac{W(r)}{r} Y_l^m \\ U_\theta &= \frac{1}{l(l+1)} \frac{d}{dr}(rW) \frac{1}{r} \frac{\partial Y_l^m}{\partial \theta} \\ U_\phi &= \frac{1}{l(l+1)} \frac{d}{dr}(rW) \frac{1}{r \sin\theta} \frac{\partial Y_l^m}{\partial \phi}. \end{aligned}\right\} \tag{4}$$

In this case, (2) is automatically satisfied and (3) becomes:

$$\mathscr{D}_l^2 W = \frac{\alpha g(r)}{\nu r} l(l+1)\tau, \tag{5}$$

where

$$\mathscr{D}_l = \frac{d^2}{dr^2} + \frac{2}{r}\frac{d}{dr} - \frac{l(l+1)}{r^2}.$$

Expressions for the viscous stresses are:

$$\left.\begin{aligned} p_{r\phi} &= \rho\nu \left[\frac{1}{r} \frac{\partial U_r}{\partial \theta} - \frac{U_\theta}{r} + \frac{\partial U}{\partial r} \right] \\ &= \rho\nu \left[\frac{d^2}{dr^2} W(r) + \frac{l(l+1)-2}{r^2} W(r) \right] \frac{\partial Y_l^m}{\partial \theta}, \\ p_{r\phi} &= \rho\nu \left[\frac{1}{r \sin\theta} \frac{\partial U_r}{\partial \theta} - \frac{U_\phi}{r} + \frac{\partial U_\phi}{\partial r} \right] \\ &= \rho\nu \left[\frac{d^2}{dr^2} W(r) + \frac{l(l+1)-2}{r^2} W(r) \right] \frac{1}{\sin\theta} \frac{\partial Y_l^m}{\partial \phi}, \end{aligned}\right\} \tag{6}$$

$$p_{rr} = 2\rho\nu \frac{\partial U_r}{\partial r} - \delta p.$$

Projection of (1) on the tangential plane of the sphere gives:

$$-\nabla_T \left(\frac{\delta P}{\rho} + \delta V \right) - \frac{\nu}{l(l+1)} \frac{d}{dr} \left[r \mathscr{D}_l W \right] \nabla_T Y_l^m = 0,$$

where the ∇_T operator has the following tangential components:

$$\left(\frac{1}{r} \frac{\partial}{\partial \theta}, \frac{1}{r \sin \theta} \frac{\partial}{\partial \phi} \right).$$

By integration on the sphere, one obtains:

$$\delta P = \frac{\nu \rho}{l(l+1)} \frac{d}{dr} (r \mathscr{D}_l W) \cdot Y_l^m - \rho \delta V$$

and finally:

$$p_{rr} = \rho \nu \left[2 \frac{d}{dr} \left(\frac{W}{r} \right) - \frac{1}{l(l+1)} \frac{d}{dr} (r \mathscr{D}_l W) \right] Y_l^m + \rho \delta V. \tag{7}$$

Equations (4), (6) and (7) allow us to write the conditions at the interfaces between layers and at the boundaries, whose explicit expressions for $W(r)$ are given in Appendix A.

In any cases U_r, U_θ, U_ϕ, $p_{r\theta}$ and $p_{r\phi}$ have to be continuous across each interface; furthermore, if an interface is crossed by the current, an additional condition concerns the continuity of p_{rr}. When the interface is a limit of two layers of convection, the interface defined by $r = r_I$ is a streamline and value of $U_r(r_I -)$ and $U_r(r_I +)$ has to be null. This last condition replaces the condition of continuity of p_{rr} and the resulting step of p_{rr} across the interface induces a deflection of the interface given by:

$$\Delta \rho_I \, \xi_I = - \frac{1}{g(r_I)} p_{rr} \Big|_{r_{I-}}^{r_{I+}}, \tag{8}$$

where $\Delta \rho_I$ is the step in density between the two layers. This deflection is due to the cumulative effect of the circulation in the two adjacent convective layers.

The top boundary located at $r = R_1$ is the lithosphere/asthenosphere interface. Two situations are considered; either a free boundary ($U_r = p_{r\theta} = p_{r\phi} = 0$) or a rigid one ($U_r = U_\theta = U_\phi = 0$). The core–mantle interface with $r = r_c$ will be a free bottom boundary ($U_r = p_{r\theta} = p_{r\phi} = 0$).

Deflection of the top boundary is given by:

$$\Delta \rho_l \xi_l = + \frac{1}{g(1)} p_{rr}(R_1),$$

and of the bottom by:

$$\Delta \rho_c \xi_c = - \frac{1}{g(r_c)} p_{rr}(R_c),$$

where $\Delta \rho_l$ and $\Delta \rho_c$ are the corresponding steps in density.

It is classical to introduce non-dimensional variables denoted by $\hat{}$ and defined by:

$$r = R_1 \hat{r}, \quad \xi = R_1 \hat{\xi}, \quad \tau = T_1 \hat{\tau}, \quad \nu = \nu_0 \hat{\nu}; \quad \rho = \rho_0 \hat{\rho}$$

and

$$W = \frac{g_0 \alpha_0 T_1 R_1^3 \, l(l+1)}{\nu_0} \hat{W}, \; V_l = 4 \pi G \rho_0 \alpha_0 T_1 R_1^2 \hat{V}_l,$$

where R_1 is the external radius of the Earth's asthenosphere; T_1 some reference

temperature; ν_0 and ρ_0 values of these quantities in the upper mantle; g_0 the value of $g(r)$, assumed constant in the whole mantle and α_0 the value of α assumed the same in every layer; V_l the harmonics component of δV.

In the following, the $\hat{}$ will be omitted and equation (5) becomes:

$$\mathscr{D}_l^2 W = \frac{\tau}{\nu r}, \tag{5'}$$

and for example, the non-dimensional $\Delta\rho_l \xi_l$ is given by:

$$\Delta\rho_l \xi_l = \alpha_0 T_1 \left[2\, l(l+1) \frac{d}{dr} \frac{W}{r} - \frac{d}{dr} (r\, \mathscr{D}_l W) \right]_{r=1} + \frac{\lambda}{2l+1} \Delta\rho_l V_l(1), \tag{10}$$

where λ is a non-dimensional parameter, defined in Appendix B.

Solution of (5′) can be written in terms of the Green's function:

$$W(r) = \int_{r_c}^{1} \mathscr{W}(r, r') \frac{\tau(r')}{\nu r'} dr', \tag{11}_1$$

where the Green's function is solution of:

$$\mathscr{D}_l^2 \mathscr{W}(r, r') = \delta(r - r') \tag{11}_2$$

and δ is the Dirac function.

Information on the computation of the Green's function is given in Appendix A.

Now ξ_l can be expressed in terms of the temperature structure by substituting equation $(11)_1$ in (10):

$$\Delta\rho_l \xi_l = \alpha_0 T_1 \int_{r_c}^{1} H_l(r')\, \tau(r')\, dr'. \tag{12}_1$$

If the disturbing gravity potential is neglected in (10), one obtains:

$$H_l(r') = \frac{1}{\nu r'} \left\{ 2\, l(l+1) \frac{d}{dr} \mathscr{W}(r, r') - \frac{d}{dr} [r\, \mathscr{D}_l \mathscr{W}(r, r')] \right\} \quad r = 1. \tag{12}_2$$

More general expressions, taking account of the disturbing gravity potential are derived in Appendix B for the H_l, H_I and H_c kernels associated with the corresponding deflections.

The component of order l of the gravity anomaly is made dimensionless by:

$$g_l = 4\pi G \rho_0 \alpha T_1 R_1 \frac{l-1}{2l+1} \hat{g}_l.$$

The gravity kernel is given by:

$$G(r') = H_l(r') + \sum_{\text{interfaces}} r_I^{l+2} H_I(r') + r_c^{l+2} H_c(r') - \alpha\rho(r')\, r'^{l+2}. \tag{13}_1$$

In the second term of this expression, one finds in order, the contribution of the top boundary, that of each internal interface, that of the bottom boundary and finally that of the density contrast due to the thermal field; one obtains:

$$\hat{g}_l = \int_{r_c}^{1} G(r')\, \tau(r')\, dr'. \tag{13}_2$$

The component of the geoid height h_l

$$h_l = V_l / g_0$$

is made dimensionless by:

$$h_l = \frac{4\pi G \rho_0 \alpha_0 T_1 R_1}{g_0} \cdot \frac{1}{2l+1} \hat{g}_l$$

and no new kernel is needed.

If the interface involves a phase change, the formalism is able to take account of the distortion of the phase boundary, coupled with the density step between phases by a condition of the type:

$$p_R(W) \Big|_{r_{I-}}^{r_{I+}} = S \cdot \tau(r_I),$$

where S is a non-dimensional number defined for example in Schubert, Yuen & Turcotte (1975). Reasonable values of physical quantities allow us to evaluate S as a few $\times 10^{-2}$ for the possible interfaces in the Earth – a negligible value – and thus this effect will not be considered further in the following.

3 Results

It is now possible to use the above formalism to obtain a better understanding of the contributions of the mantle convection to both gravity and residual depth anomalies. Although the formalism allows us to consider several transition layers, we propose to limit ourselves to one transition only; that associated with the spinel–post-spinel transition layer at 650–700 km depth, classically considered as the interface between the upper and lower mantles.

This transition could have a notable influence on the circulation and thus inferred gravity by its possible role as a lower limit for the Benioff planes and as a boundary of two distinct geochemical reservoirs (Richter & McKenzie 1981).

An insight into this problem will be obtained by considering only cases with two layers; the possible patterns of the mantle convection will be studied by the choice of three major items:

the dynamical coupling with the top plate: free (F) or rigid (R);

a step of viscosity between the upper and lower mantle (N, if no step, S for a step);

one layer of convection in the whole mantle (O) or two layers, one in the upper, the other in the lower mantle (T).

This leads us to consider eight cases; each one is defined by three letters, for example, FSO is the case with a free top boundary, a step of viscosity across the post-spinel interface and only one layer of convection in the whole mantle.

Let us consider the ratio of the lower mantle viscosity over the upper mantle one; a rapid increase of the viscosity of the mantle with depth (involving a value 10^4–10^6 of this ratio) was later supported by authors who interpreted the equatorial bulge of the Earth's figure as a fossil bulge but now, from different considerations, the range of possible value of this ratio is believed more limited (between 1 and 100) and even, from an isostatic rebound model, close to one (Peltier 1976, I and II).

For the item 'S', the value of 100 for this ratio will be generally adopted, but in Fig. 3 the intermediate value of 10 is also considered.

Values of the physical parameters are shown in Table 1. In Fig. 1 are drawn the gravity and height kernels for four chosen values of l:

$l = 2$ and 3, main values concerned by the planetary scale convection;

$l = 6$, typical of the plate scale convection with a half-wavelength of 3333 km;

$l = 30$, associated to small aspect ratio convective cells in the upper mantle, with a half-wavelength of 667 km.

Parsons & Daly (1984) have made a very similar analysis in a planar two-dimensional geometry with a single layer of convection. The comparison of their results with ours, when possible, is very good and is shown in Table 2.

Table 1. Numerical value of the physical parameters adopted in this study – indexes c, 1, 2, I are relative to the core, lower and upper mantles and the lithosphere, respectively; value of γ from Schubert *et al.* (1975).

	Physical parameter	Value	Non-dimensional value
g_0	Value of the Earth gravity in the whole mantle	$10\ \mathrm{m\ s^{-2}}$	
ν_1	Kinematic viscosity in the lower mantle	ν_2 or $100\ \nu_2$	1 or 100
ν_2	Kinematic viscosity in the lower mantle		
α_0	Coefficient of volumic expansion	$3.31 \times 10^{-5}\ ^\circ\mathrm{C}^{-1}$	
$\rho_0 (= \rho_\mathrm{m})$	Density in the mean mantle	$4.5 \times 10^3\ \mathrm{kg\ m^{-3}}$	
$\Delta\rho_\mathrm{I}$	$\rho_1 - \rho_2$ difference density between lower and upper mantle	$0.4 \times 10^{-3}\ \mathrm{kg\ m^{-3}}$	
$\Delta\rho_\mathrm{c}$	$\rho_\mathrm{c} - \rho_\mathrm{m}$	$6.5 \times 10^3\ \mathrm{kg\ m^{-3}}$ (for the computation of S) 0 (for the computation of $H_1, H_\mathrm{I}, H_\mathrm{c}$)	
R_1	External radius of the Earth's asthenosphere	6.271×10^6 m	1
R_I	Radius of the interface lower/upper mantle	5.721×10^6 m	0.9123 (r_I)
R_c	Radius of the Earth's core	3.479×10^6 m	0.5548 (r_c)
β	Temperature gradient	$10^{-3}\ ^\circ\mathrm{C\ m^{-1}}$	
γ	Slope of the Clapeyron curve at the post-spinel interface	-1.3×10^6 pascal $\mathrm{m^{-1}}$	
S	Dimensionless parameter, measure of the importance of the phase change instability to the Rayleigh one		-2×10^{-2}

3.1 REQUIREMENTS ON THERMAL PROFILES

For a component of the thermal field in $\tau(r)\ Y_l^m(\theta, \phi)$, with $\tau(r) > 0$, ascending hot limbs are centred over maxima of Y_l^m and descending cold limbs over minima. For this reason and at least for the fundamental wavelength component associated with a given convective pattern, $\tau(r)$ apparently keeps the same sign in a whole stage of convection and is of the opposite sign inside adjacent layers.

Generalization of these considerations to the harmonic components is questionable. The results shown in Fig. 7 of Parsons & Daly (1984) seem in favour of this generalization but our experiment, for a set of completely different cases, does not (Rabinowicz *et al.* 1983).

Let us now define the function $S(r)$ by:

case O (one convective layer): $S(r) = +1$ in the whole mantle,

case T (two convective layers): $S(r) = +1$ in the upper mantle,

$S(r) = -1$ in the lower mantle.

Above considerations allow us to write:

$$S(r)\,\tau(r) \geqslant 0. \qquad \text{(A)}$$

Table 2. Comparison of the cases FF and RF from Parsons & Daly (1984), involving a free bottom and a free or rigid top boundary with our cases FNO and RNO, respectively. In our two cases, and for each l, the kernel G, null at $r = r_c$ and $r = 1$ achieves a maximum value, showed in the second column (for each l, up: case FNO, down: case RNO). The same behaviour is seen for Parson's results. For each l, the associated value of the wavelength $\lambda = (40 \times 10^6 \text{ m})/l$ allows us to compute an aspect ratio λ/d (column 3), where d is the thickness of the mantle $(R_1 - R_c)$ and the closest value of this ratio in Parson's study can often be found (column 4). The corresponding maximum of G is given in column 5 (up: case FF comparable to our FNO, down: case RF comparable to our RNO). The comparison shown by the extrema values of the kernel G can be considered as very good, proving that the change of planar by spherical geometry is of limited importance but the factor $(l-1)/(2l+1)$ must not be forgotten in the dimensioned quantity.

l	Extrema of G FNO / RNO	λ/d	Closest value of λ/d in Parson's study	Extrema of G FF / RF
2	0.13 0.30	7.2	8	0.15 0.38
3	0.20 0.34	4.8	–	– –
6	0.29 0.37	2.4	2	0.3 –
30	0.35 0.36	0.48	0.4	0.4 –

This gives to $S(r)$ the meaning of the required sign of any acceptable thermal component at the radius r for the fundamental mode.

Let us assume that the thermal profile verifies (A). Then interesting conclusions can be derived considering the kernels associated with each l value, as shown in Fig. 1.

3.2 CONCLUSION 1

In every case, the contribution due to the deflection of the interface core/mantle to the gravity anomaly is either small for $l = 2$ and 3 (less than 10 per cent) or very small for $l = 6$ (less than 1 per cent) to completely negligible for $l = 30$.

3.3 CONCLUSION 2

For $l = 30$, any contribution of the lower mantle to both the lithospheric deflection and gravity anomaly is at most small and even negligible from the deep part. Changes in the value of the viscosity step, of the number of convective layers and, to a lesser extent, of the dynamical top boundary condition modify the relative importance of the gravimetric contributions for $l = 30$ but notably less than in cases relative to a small value of l. Similarly, negative values of the admittance are never achieved for $l = 30$.

Figure 1. For each case and for the values of $l = 2$, 3, 6 and 30 are shown the following kernels: (a) contribution to the total gravity kernel G of the deflection of the top boundary; (b) contribution to G of the interface upper–lower mantle, only given when non-null (two layers of convection); (c) contribution to G of the interface mantle–core (the bottom boundary); (d) contribution to G of the thermal density contrast; (e) G itself.

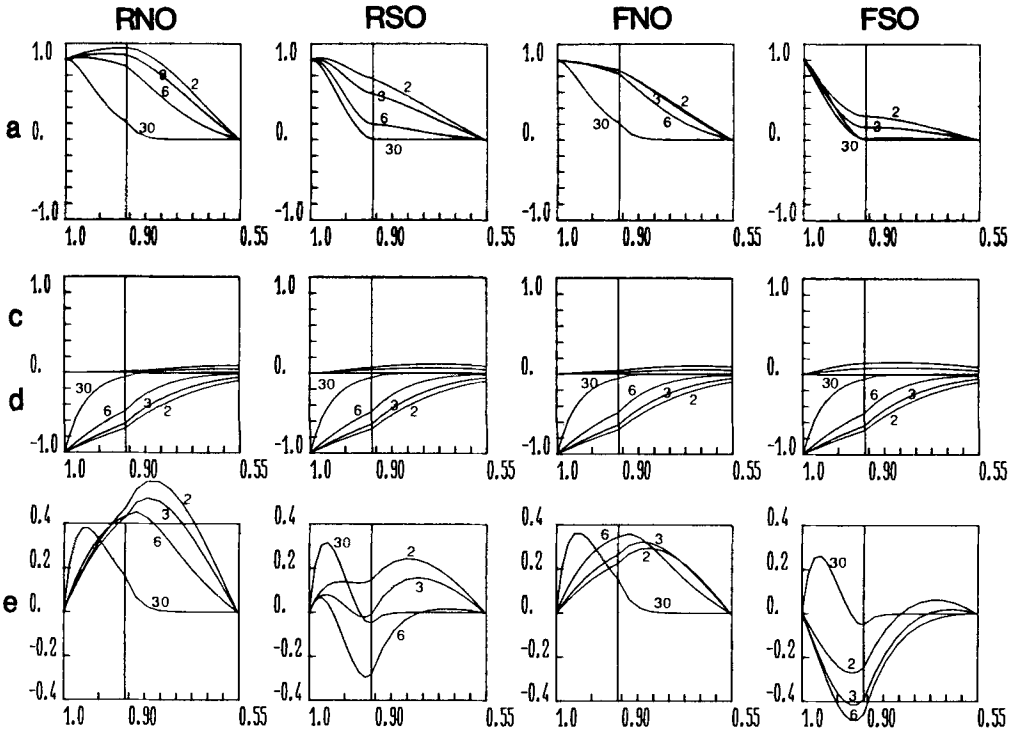

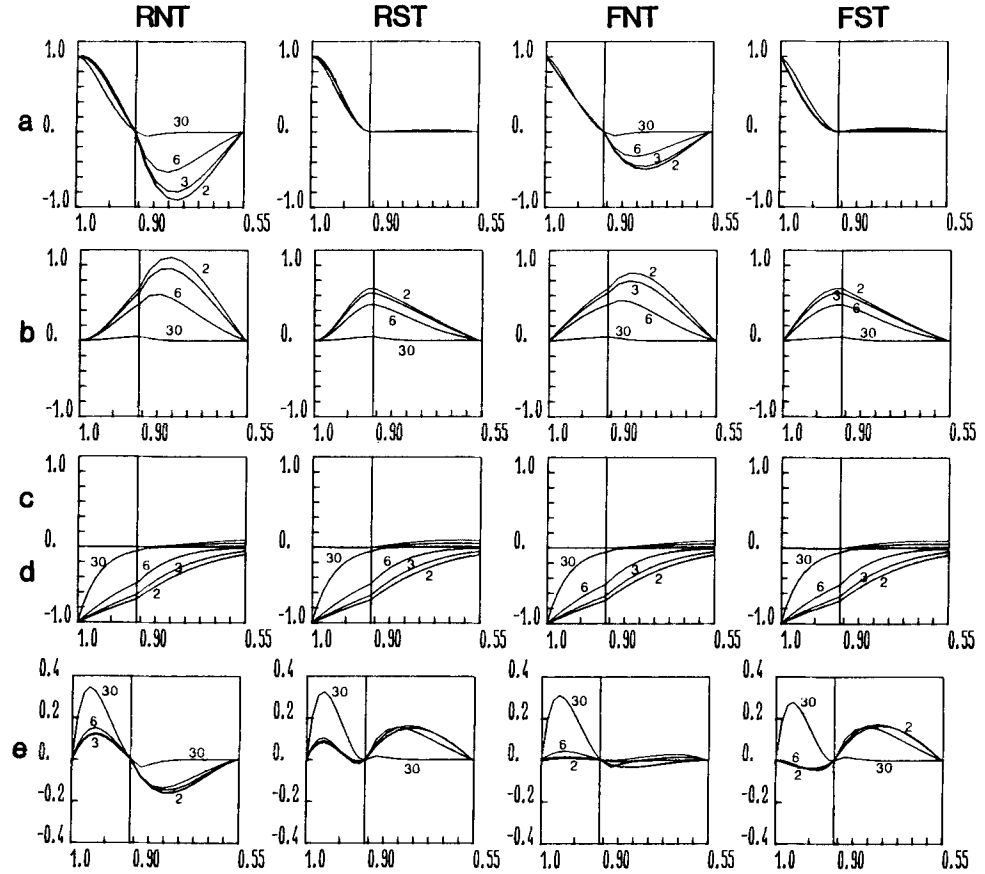

3.4 CONCLUSION 3

As noted by Hager (1982), the gravitational effects of the surface deformation and the driving density contrast are of comparable magnitude and opposite sign and nearly cancel. This is illustrated in the cases with only one convective layer, where deflection of the upper–lower mantle interface is null and those of the core–mantle interface gives negligible contribution (conclusion 1), leaving alone the contributions of the lithospheric deflection and of the thermal density contrast; in order to evaluate the cancelling effect, one may choose the quotient of the extrema values for r in the range $(r_c, 1)$, of the two kernels

$$\frac{\text{Sup}\,|G|}{\text{Sup}\,|H_l|}$$

to be rarely bigger than 0.15.

In cases involving two layers of convection, the positive contribution due to the deflection of the upper–lower mantle interface is notable and has to be added to those of the lithospheric deflection before getting a sum of comparable magnitude with the effect of the thermal density contrast.

3.5 CONCLUSION 4

As an *a posteriori* statement, the kernel $H_l(r')$ has in every case and for the whole range of r', the same sign as $S(r')$. This can be written:

$$H_l(r') \cdot S(r') \geqslant 0.$$

This point has an important consequence: for any acceptable thermal profile, verifying condition (A), every contribution of any elementary layer gives a positive contribution to ξ.

3.6 CONCLUSION 5

Concerning G, it can have the same sign of S or not. More precisely, let us define the sub-interval I of $\{r_c, 1\}$ of value r' giving a negative contribution to the admittance such that $r' \in I$ if and only if:

$$G(r') \cdot S(r') \leqslant 0.$$

Table 3 shows the sub-interval I for every case. Three situations are possible:

(a) $I = \phi$ (the void set). This occurs in cases R or F, N, O (every l); R, N, T (every l); F, N, T ($l = 6$ and 30) and also R, S, O ($l = 2$).

In such cases and for the very large class of acceptable thermal profiles, verifying condition (A), every contribution to Δg_T from every elementary layer is positive and the admittance is always positive.

Table 3. Sub-interval I for every case – ϕ holds for the void set. In the definition of a given case: R is for a rigid top boundary, F for a free one; N for a condition of no step of viscosity, S for a factor 100 between viscosities of the upper and lower mantles; O for one convection layer and T for two layers.

Case \ l	2	3	6	30
RNO	ϕ	ϕ	ϕ	ϕ
FNO	ϕ	ϕ	ϕ	ϕ
RSO	ϕ	0.90, 0.94	0.74, 0.965	r_c, 0.925
FSO	0.79, 1	0.70, 1	r_c, 1	r_c, 0.94
RNT	ϕ	ϕ	ϕ	ϕ
FNT	r_c, 0.84	r_c, 0.76	ϕ	ϕ
RST	r_c, 0.93	r_c, 0.93	r_c, 0.93	r_c, 0.91
FST	r_c, 1	r_c, 1	r_c, 1	r_c, 0.91

(b) $I = \{r_c, 1\}$ this occurs in cases FST (for $l = 2, 3, 6$) and FSO ($l = 6$). One gets the inverse result from (a). For the same class of acceptable thermal profiles, every contribution to Δg_T is negative and so is the admittance.

(c) $I \neq 0$ and $\neq \{r_c, 1\}$. In such a case it is possible to get either positive or negative value of Δg_T and of the admittance, according to the details of the particular thermal profile. Negative admittances need relatively larger values of $\tau(r)$ inside I than outside. A negative value of the admittance is likely to be found in case FSO ($l = 2, 3$) if the driving density contrast is essentially in the upper mantle and alternatively for the cases RST ($l = 2$, 3 or 6) (*cf.* Fig. 5b) and FNT ($l = 2, 3$) (*cf.* Fig. 5a) if this same contrast is preferentially in the lower mantle. But, of course, such a situation can favour small or even very small positive or negative value of the admittance. These points are illustrated in Figs 2–5, involving a choice of a few examples of different acceptable thermal profiles.

For the value $l = 30$, despite a large interval I for some cases, the deep localization of this interval and the small value of G_{30} normally prevent a negative value of the admittance (*cf.* Figs 2–5).

For the value $l = 6$, the conclusions are easily outlined: positive admittances are always found if no step of viscosity occurs; if a step of viscosity is associated with a free top boundary (cases F, S, O or T), negative admittance is certain; if a step of viscosity is associated with a rigid top boundary (cases R, S, O or T), to get this negative value, the thermal driving contrast must be deep enough.

With a few modification, the same kind of conclusions are also valid for $l = 2$ and 3. However, the negative admittance is still more difficult to achieve with a rigid top boundary and may even be impossible (case R, S, O, $l = 2$). With two layers of convection and without a viscosity step, the admittance is in any case very small for $l = 2$ and 3.

4 Geophysical implications

In a former study (Rabinowicz *et al.* 1983, hereafter denoted paper I), mean gravity profiles across Central and South America and Eurasia in the direction normal to the subduction zones deduced from the GEM 10B gravity models have been computed (see Fig. 6): a strong similarity between these profiles can be noted. There exists:

a linear slope towards the interrior of the plate;

an absolute maximum close to and landward of the trench;

an absolute minimum at a distance of the order of 3500 km from the trench, followed by a small secondary maximum correlated positively with swells like the Bermuda Rise for Central America, or the Rio Grande at the latitude of Chile.

Such a shape has been interpreted in paper I as a consequence of a large convective cell driven by the subducting slab acting as a heat sink.

When an oceanic slab subducts at an age of about 100 Myr, it has been considerably cooled by a mean value of 600°C over a depth of 60 km: the energy needed in order to warm it again is huge: 10^5 W s^{-1} for each metre of trench line, equivalent to the total heat production in the Earth along a section of 2000 km. A set of 2-D numerical convective models in the upper mantle in a vertical plane at right angles to the azimuth of the trench, incorporating the cooling action of the sinking slab by a cold vertical wall, shows the formation of a very large convective cell flowing downward along the cold interface of the sinking slab, and next horizontally along the post-spinel interface, before rising again 3000 km away (Fig. 7) (Rabinowicz *et al.* 1980).

We will now try to prove that most of the gravity signal landward of the trench can be the surface manifestation of the large convective cell driven by the sinking slab. Let us take

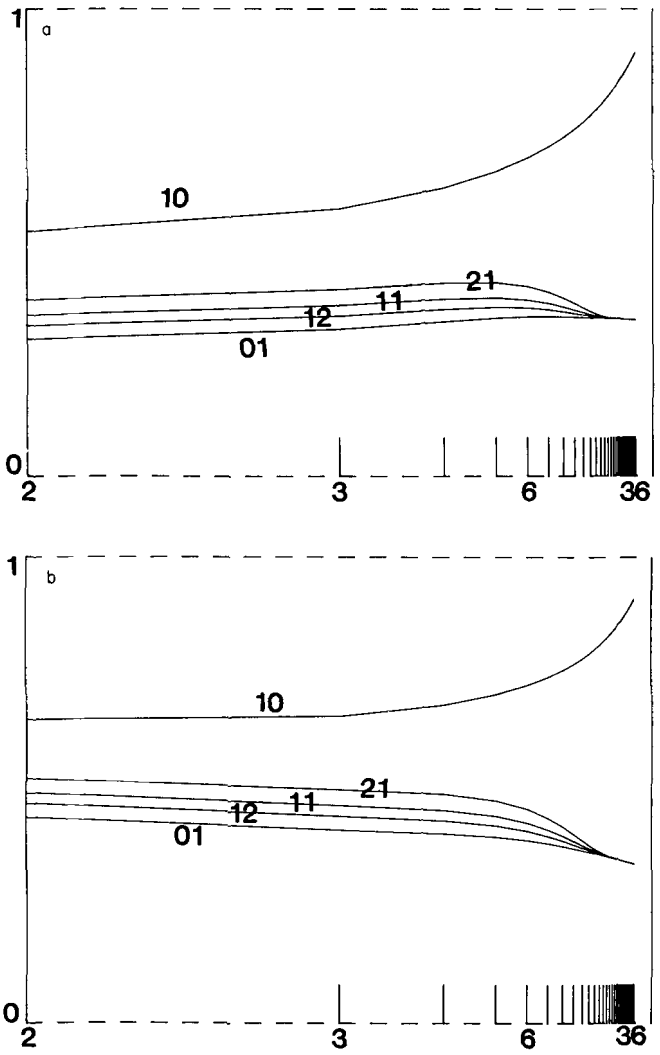

Figure 2. Non-dimensional admittance versus l for a one-layer convection across the whole mantle with constant viscosity. In (a) the top boundary is free (case FNO), in (b) it is rigid (case RNO). Different conductive thermal profiles are used, solution of $\mathscr{D}_l(\tau) = 0$ with non-dimensional $\tau(1) = m_1$ and $\tau(r_c) = m_2$.

$$\tau = \frac{(m_1 - m_2 r_c^{l+1})\, r^l + [-m_1 r_c^{l+1} + m_2 r_c^{l+1}]\, r^{-l-1}}{1 - r_c^{2l+1}} .$$

Five cases whose values of m_1 and m_2 are (1, 0), (2, 1), (1, 1), (1, 2) and (0, 1) respectively, relative to an increasingly deep driving thermal contrast, are presented. The deeper the thermal contrast, the smaller is the admittance which always stays positive; the value being a little larger for a rigid top boundary than for a free one. With the exception of the first case (1, 0), all the profiles are very close and have a common asymptotic value for large l of about 0.35; this statement is still true in the other figures.

into consideration, for example, the case of Central America (see Fig. 8) and propose, in accordance with the above remarks, that the flow driven by the sinking slab moves away normally to the Middle America trench, along the bottom of the upper mantle, crosses successively Honduras, Cuba, Bahama and ascends under the Bermuda swell, located at

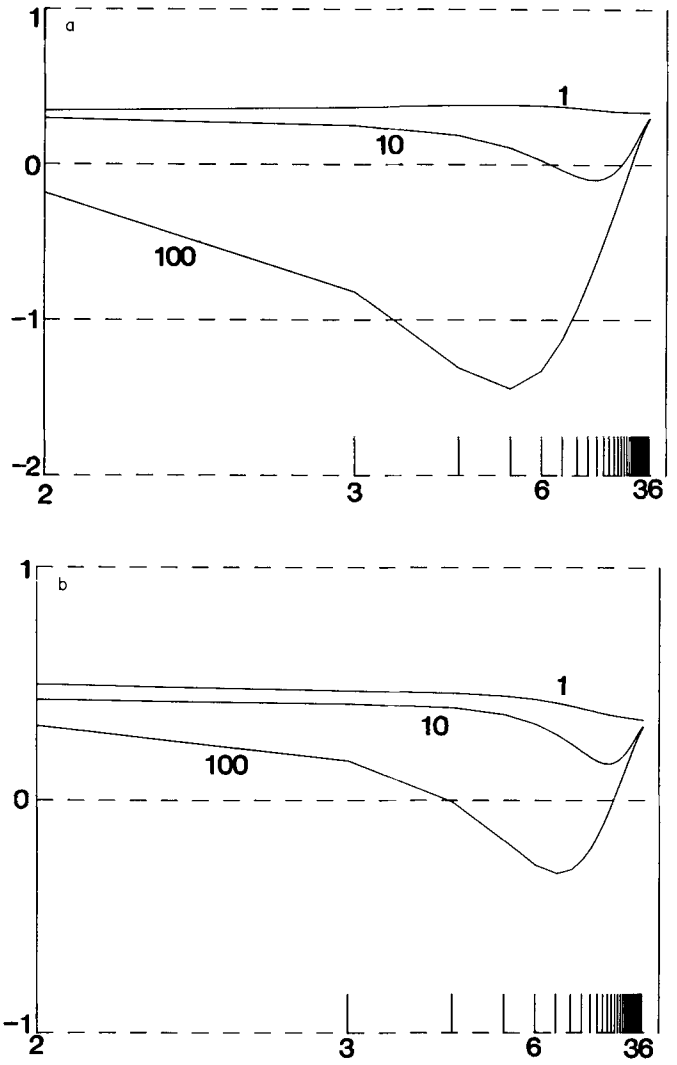

Figure 3. Non-dimensional admittance for a one-stage convection with an increasing value of the viscosity ratio ν_2/ν_1 equal to 1, 10 and 100. Same definition of the trial thermal function as in Fig. 2 with $m_1 = m_2 = 1$. (a) and (b) are relative to cases FSO and RSO respectively. The increase of the viscosity ratio favours a decrease of the admittance chiefly for values of l close to 6 but the negative values are more easily achieved with a free top boundary.

4000 km from the trench. Now, one has to check if the gravity and topography data are compatible with results of our models.

Since the sediment and crustal thicknesses over most of these regions hide most of the dynamical deflection of the lithosphere due to the convection, one is unable to compute the value of the admittance. However, in the vicinity of the subduction slab, one can assert that the long-wave component of the temperature field and of the observed gravity anomaly reach respectively a minimum and a maximum close to the subducting plane, inferring that the unknown dynamical contribution to the gravity field is weaker than the one due to the thermal field, from which one infers a negative value of admittance.

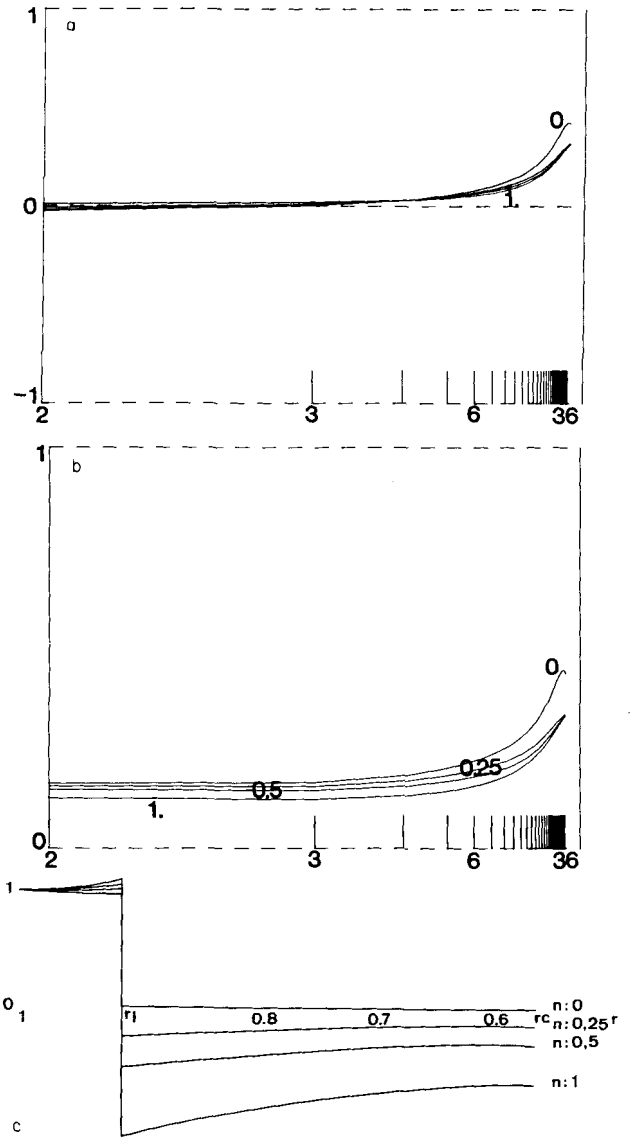

Figure 4. Non-dimensional admittance for a two-stage convection in the mantle with constant viscosity; (a) and (b) are relative to cases FNT, RNT respectively. The physical situation involving the localization of the hot and cold currents in each layer and the pressure of two thermal boundary layers on both sides of the interface (see text) leads us to impose the following condition for the trial thermal function: $\tau(r_{I-}) + n\,\tau(r_{I+}) = 0$;

$$\left[\frac{d\tau}{dr}\right]_{r_{I-}}^{r_{I+}} = 0;\quad \frac{d\tau}{dr}(r_c) = 0$$

and $\tau(1) = 1$. Thus, $\tau(r) = k(a_+ r^l + b_+ r^{-l-1})$ for $r_I \leqslant r \leqslant 1$ and $k(a_- r^l + b_- r^{-l-1})$ for $r_c \leqslant r \leqslant r_I$ with

$$a_+ = l(1-n) + 1 + (1+n)l\,(r_c/r_I)^{2l+1}$$

$$b_+ = l(1+n)\,r_I^{2l+1} + l/l + 1 - n\,r_c^{2l+1}$$

$$a_- = -(2l+1)\,n,\quad b_- = -\frac{(2l+1)\,l}{l+1}\,r_c^{2l+1}$$

and $k = 1/(a_+ - b_+)$. These functions are shown for $l = 2$ (c). The values of n have to be positive in order to satisfy condition (A) of Section 3; the proposed values of n are 0, 0.25, 0.5, 1. The admittance is quasi-null of $l \leqslant 8$ for a free top boundary in agreement with the very small amplitude of the corresponding G kernel (case FNT of Fig. 1).

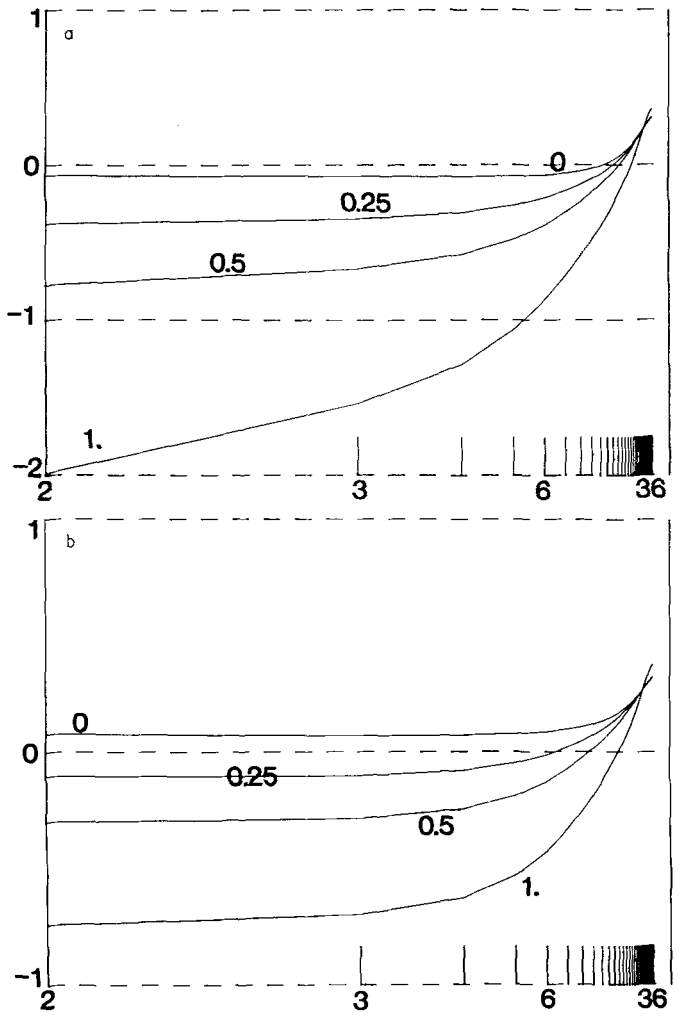

Figure 5. The same situation as in Fig. 4 but with a ratio of viscosity ν_2/ν_1 of 100 (a) and (b) are relative to cases FST and RST respectively. Negative values of the admittance for $l \leqslant 8$ are now easily achieved as soon as the thermal contrast concerns the lower mantle but, as usual, more easily with a free top boundary than with a rigid one.

Gravity associated with the 2-D upper mantle flow model of Fig. 7 has been studied in detail in paper I (see Fig. 9). We have found that a negative admittance is achieved if the following boundary conditions are assumed: a free coupling with the top boundary and a rigid or semi-deformed lower interface. For such cases, the model is able to reproduce correctly the shape of the observed profiles: the long-wave decreasing slope away from the subduction zone; the local maxima of gravity observed over the Bermuda swell.

Let us now consider the convective mode directly comparable to the large convective flow described above; it involves two layers of convection and a value of l equal to 6, corresponding to cells of 3300 km of horizontal extent. In such a case, the conditions favouring a negative admittance are:

a free coupling with the top;
an increase of viscosity across the post-spinel interface;
eventually a deep thermal contrast.

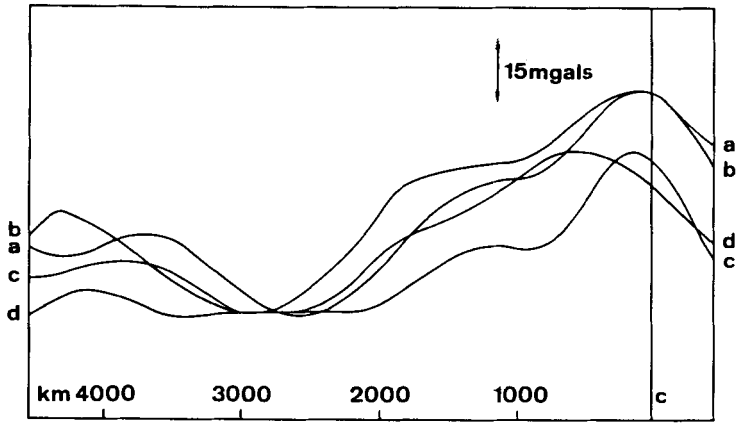

Figure 6. Average gravity profiles normal to the subduction (right) to the interior of the plate (left) and across (a) Central America; (b) South America at the Peru latitude; (c) South America at the Chile latitude; (d) eastern Asia (from paper I). For (a), (b) and (c), the geographical direction has been reserved for comparison.

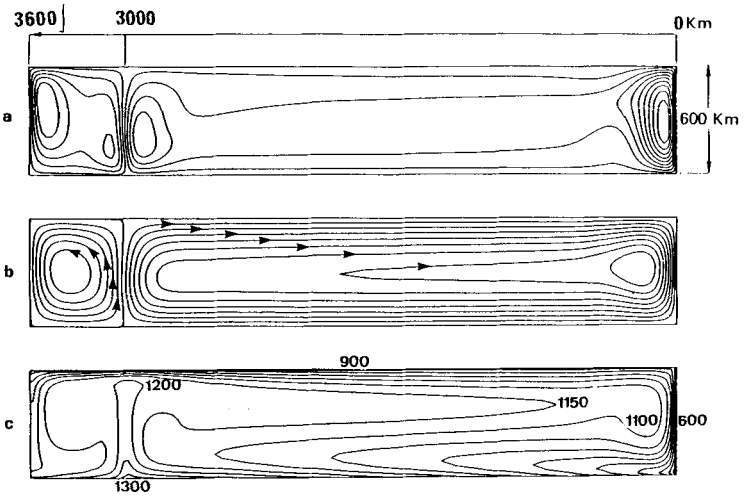

Figure 7. Isovorticity lines (a), streamlines (b), isotherms (c) for a convective circulation model; computation made in a $3600 \times 600\,km^2$ box with a regular 150×25 meshing (from Rabinowicz *et al.* 1980).

A good analogy can be established between the conditions needed respectively by the former and present studies. The condition of a free top boundary is directly comparable; a big increase in viscosity can be considered as nearly analogous to a rigid coupling at the bottom of the upper mantle; a powerful motor in the deep mantle induced by a deep thermal contrast is a way to counteract the dynamical effect of the upper mantle circulation on this same interface, achieved in paper I by a condition of semi-deformed or undeformed bottom face.

With these interpretations in mind, the comparison is good, but the present study allows us to be more precise. For example, if our interpretation of the gravity profiles across Central and South America and Eurasia is correct, a constant value of the viscosity in the whole mantle can be ruled out for any choice of the number of layers of convection.

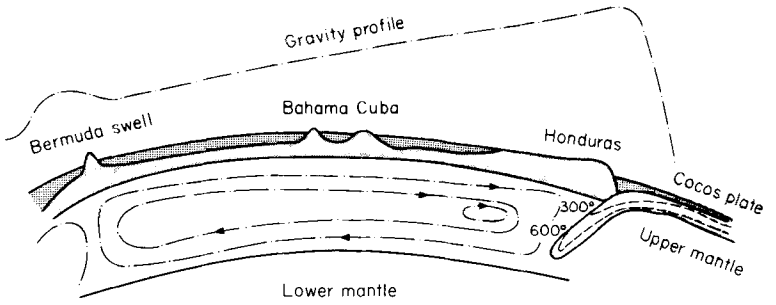

Figure 8. Geophysical interpretation of the mean gravity profile across Central America.

Thus a big enough increase of viscosity versus depth of at least one order of magnitude and more likely of two orders seems needed. It can be progressive or steep, but it must concern a transition zone between the upper and lower mantles.

This conclusion is not significantly affected by the absence of knowledge of the true temperature profile and as an interesting corollary its validity seems independent of the value of the Rayleigh number. This gain is due to the consideration of the height and gravity kernels; meanwhile, one must not forget the need of the condition (A) on the thermal profile and the possible limitation of the conclusions to the only fundamental component.

Let us outline the limitations and difficulties of the study with regard to the data, the concern as mentioned before is the absence of observational data on the lithospheric deflection in any continental area and *de facto* in large parts of oceanic areas. But more important, one must assume that gravity, geoid and residual depth anomaly profiles are due to a common dynamical cause and not to a large wavelength thickness of the crust or any similar static cause (McNutt 1980; Rabinowicz & Lago 1984). Such an assumption seems more valid as the wavelength becomes larger, implying a greater importance for the first harmonic of the Earth's gravity field.

5 Other geophysical considerations

We have no reason to limit our interest to the case $l = 6$. The value $l = 30$ corresponds to convective cells of aspect ratio close to 1 in the upper mantle. In such a case, our results do not differ from planar 2-D ones (McKenzie *et al.* 1980). To illustrate the possibility of the cases ($l = 2$ and 3), one can consider the results obtained by Menard & Dorman (1977). Taking into account the fact that the ridge crests are roughly 700 m deeper at the equator than they are in the high northern latitudes, they attempted an exhaustive study of latitudinal variations in depth of the ridge crests of every ocean. As a result, they get a determination of two non-zero admittances of $-0.039\,\text{mgal}\,\text{m}^{-1}$ for $l = 2$, using for Δg_2 the difference between the terms of the Earth potential and those of the reference ellipsoid and of $0.029\,\text{mgal}\,\text{m}^{-1}$ for $l = 3$. Let us note that these admittances strictly concern purely zonal terms and are deduced from data observed only in the vicinity of ridges; thus, they are not valid globally. Associated non-dimensional values of the admittance are -0.975 for $l = 2$ and $+0.332$ for $l = 3$. They are very different values, never simultaneously found for value $l = 2$ and 3 in the cases shown in Figs 2–5. To solve the difficulty, one can adopt only one of these values to account for mantle circulation of the kind studied in Section 3.

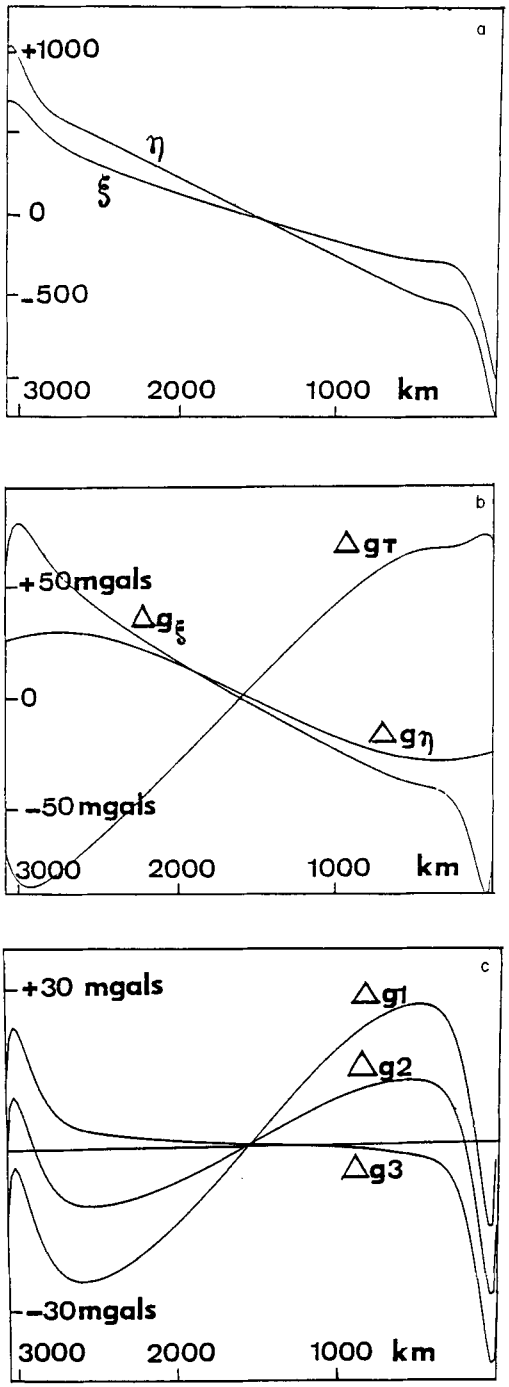

Figure 9. For the large right cell of the model presented in Fig. 7. (a) ξ and η, deflections of the upper and lower faces respectively of the cavity due to dynamical effects; normalized values are computed with a density contrast across the interface equal to ρ, the density of the upper mantle. (b) Δg_ξ, Δg_η and Δg_T are contributions to the anomaly of gravity of the ξ and η deflections respectively and the thermal field. (c) Δg_1, Δg_2 and Δg_3, global gravity profiles with the undeformed, semi-deformed and deformed bottom face conditions respectively.

Let us start by adopting $l = 2$, the contribution in $l = 3$ is then likely to be considered as a simple harmonic, just able to modulate a geometric pattern of a circulation essentially governed by a $P_{2,0}$ term. This point of view favours our former conclusion of an increase of the viscosity versus depth.

Alternatively, $l = 3$ can be adopted; in such a case, the term $l = 2$ can probably be governed by the circulation in the core and/or by the distortion of the core–mantle interface. Another possibility, often invoked 10 to 20 years ago, considers the excess of the measured second zonal harmonic as indicating that the mantle possesses a memory for the faster rotation of the Earth in the past. This statement has been proved untrue by Goldreich & Toomre (1969). In any case, if the value of the admittance given by the order 3 is considered as an answer to mantle circulations it is difficult, but not impossible, to balance this point of view with an increase in viscosity with depth (see Fig. 3b).

In conclusion, this first short analysis of the known data at present in the light of the theory given above allows us to propose:

long-wavelength gravity, geoid and residual depth anomaly profiles are able to give an insight into the behaviour of the viscosity of the mantle versus depth;

these same profiles are less able to select between a one-layer or a two-layer convective circulation in the Earth's mantle,

If one is confident in our interpretation of mean gravity profiles across continental plates normal to the trench line, one is lead to adopt an increase in the viscosity of at least one order of magnitude between the upper and lower mantle.

References

Chandrasekhar, S., 1961. *Hydrodynamic and Hydromagnetic Stability,* Oxford University Press.

Hager, B. H., 1982. The geoid and geodynamics, *Nature,* **299,** 104–105.

Goldreich, P. & Toomre, A., 1969. Some remarks on polar wandering, *J. geophys. Res.,* **74,** 2555–2567.

Kaula, W. H., 1972. Global gravity and mantle convection, in *The Upper Mantle,* ed. Ritsema, A. R., *Tectonophys.,* **13,** 341–359.

McKenzie, D., 1977. Surface deformation, gravity anomalies and convection, *Geophys. J. R. astr. Soc.,* **48,** 211–238.

McKenzie, D., Watts, A., Parsons, B. & Roufosse, M., 1980. Planform of mantle convection beneath the Pacific Ocean, *Nature,* **288,** 442–446.

McNutt, M., 1980. Implications of regional gravity for state of stress in the Earth's crust and upper mantle, *J. geophys. Res.,* **85,** 6377–6396.

Menard, H. W. & Dorman, L. M., 1977. Dependence of depth anomalies upon latitute and plate motion, *J. geophys. Res.,* **82,** 5329–5335.

Nataf, H. C., Froidevaux, C., Levrat, J. L. & Rabinowicz, M., 1981. Laboratory convection experiments: effect of lateral cooling and generation of instabilities in the horizontal boundary layers, *J. geophys. Res.,* **86,** 6143–6154.

Parsons, B. & Daly, S., 1984. The relationship between surface topography, gravity anomalies and the temperature structure of convection, *J. geophys. Res.,* in press.

Peltier, W. R. & Andrews, J. T., 1976. Glacial isostatic adjustment – I, The forward problem, *Geophys. J. R. astr. Soc.,* **46,** 605–646.

Rabinowicz, M. & Lago, B., 1984. Large scale gravity profiles as evidences of a convective circulation, *Terra Cognita,* in press.

Rabinowicz, M., Lago, B. & Froidevaux, C., 1980. Thermal transfer between the continental asthenosphere and oceanic subducting lithosphere: its effects on subcontinental convection, *J. geophys. Res.,* **85,** 1839–1853.

Rabinowicz, M., Lago, B. & Souriau, M., 1983. Large-scale gravity profiles across subducted plates, *Geophys. J. R. astr. Soc.,* **73,** 325–349.

Ricard, Y., Fleitout, L. & Froidevaux, C., 1984. Geoid heights and lithospheric stresses for a dynamical earth, *Annls Géophys.,* in press.

Richter, F. M. & McKenzie, D. P., 1981. On some consequences and possible causes of layered mantle convection, *J. geophys. Res.*, **86**, 6133–6142.

Runcorn, S. K., 1972. Dynamical processes in the deeper mantle, in *The Upper Mantle*, ed. Ritsema, A. R., *Tectonophys.*, **13**, 623–637.

Sandwell, D. T., 1982. Thermal isostasy: response of a moring lithosphere to a distributed heat source, *J. geophys. Res.*, **87**, 1001–1014.

Schubert, G. & Turcotte, T. L., 1971. Phase changes and mantle convection, *J. geophys. Res.*, **76**, 1424–1432.

Schubert, G., Yuen, D. A. & Turcotte, D. L., 1975. Role of phase transition in a dynamic mantle, *Geophys. J. R. astr. Soc.*, **42**, 705–735.

Watts, A. B., 1976. Gravity and bathymetry in the Central Pacific Ocean, *J. geophys. Res.*, **81**, 1533–1553.

Watts, A. B., 1978. An analysis of isostasy in the World's ocean 1. Hawaiian-Emperor Seamount Chain, *J. geophys. Res.*, **83**, 5989–6004.

Appendix A

Only cases with two layers will be considered in this appendix. Green's function is the solution of $(11)_2$:

$$\mathscr{D}_l^2 \, \mathscr{W}(r, r') = \delta(r - r'). \tag{A1}$$

For a given value of r', one has to solve the equation:

$$\mathscr{D}_l^2 \, \mathscr{W}(r, r') = 0, \tag{A2}$$

in three layers, involving the two interfaces defined by $r = r_I$ and $r = r'$ (r' is assumed to be different from r_I but can be equal to $r_I + \epsilon$ or $r_I - \epsilon$).

In each layer, a determination of $\tau(r, r')$ is obtained of the form:

$$A_c r^l + B_c r^{-l-1} + C_c r^{l+2} + D_c r^{-l+1} \tag{A3}$$

for the general solution of (A2) where the coefficients depend on r'; $c = 1, 2, 3$ are associated to each layer with an increasing value from inside to outside.

Conditions at the interface r' are given by the presence of the Dirac function:

$$\mathscr{W}(r, r') \Big|_{r'-}^{r'+} = \frac{d\mathscr{W}}{dr} \Big|_{r'-}^{r'+} = \frac{d^2\mathscr{W}}{dr^2} \Big|_{r'-}^{r'+} = 0 \tag{A4}$$

and

$$\frac{d^3\mathscr{W}}{dr^3} \Big|_{r'-}^{r'+} = 1.$$

In the case of an interface crossed by the current (cases with one layer of convection), conditions at the interface r_I are given by:

$$\mathscr{W} \Big|_{r_I-}^{r_I+} = \frac{d\mathscr{W}}{dr} \Big|_{r_I-}^{r_I+} = P_T(\mathscr{W}) \Big|_{r_I-}^{r_I+} = P_R(\mathscr{W}) \Big|_{r_I-}^{r_I+} = 0, \tag{A5a}$$

where

$$\left.\begin{aligned} P_T(\mathscr{W}) &= (\rho\nu)\, r' \left[\frac{d^2\mathscr{W}}{dr^2} + \frac{l(l+1)-2}{r^2}\right] \\ \text{and} \qquad & \\ P_R(\mathscr{W}) &= (\rho\nu)\,(r') \left[2l(l+1)\frac{d}{dr}\frac{\mathscr{W}}{r} - \frac{d}{dr}(r\mathscr{D}_l\mathscr{W})\right] \end{aligned}\right\}. \tag{A6}$$

If the interface is limit of two adjacent layers of convection, the last condition (A5a) is replaced by:

$$\mathscr{W}(r_{I-}, r') = \mathscr{W}(r_{I+}, r') = 0. \tag{A5b}$$

Boundary conditions are:

$$\mathscr{W}(1, r') = \mathscr{W}(r_c, r') = \frac{d^2\mathscr{W}(r_c, r')}{dr^2} = 0 \tag{A7}$$

and

$$\frac{d^2}{dr^2}\mathscr{W}(1, r') = 0$$

for a free top boundary or

$$\frac{d}{dr}\mathscr{W}(1, r') = 0$$

for a rigid top boundary.

The 12 conditions given by (A4), (A5) and (A7) constitute a linear system, whose solution gives the value of the 12 unknowns A_c, B_c, D_c for any given value of r'.

Value of the different kernels at this value r' are easily obtained; one gets, for example from $(12)_2$:

$$H_l^*(r') = \frac{2}{\nu r'}\, l(l+1)\,[(l-1)A_3 - (l+2)B_3] + [l^2 - l - 3]\,(l+1)\,G_3 - [l^2 + 3l - 1]\,lD_3]$$

where the following formula has been used:

$$\mathscr{D}_l\, r^k = [k(k+1) - l(l+1)]\, r^{k-2}.$$

Appendix B

By taking account of the contribution of the disturbing gravity potential in the computation of the kernels, it follows from equation (10) that:

$$H_l(r') = H_l^*(r') + \lambda\Delta\rho_l \left[\frac{H_l + H_I r_I^{l+2} + H_c r_c^{l+2}}{2l+1} - \alpha\rho(r')\, V_l(1, r)\right] \tag{B1}$$

where H_l^* is the expression of the second member of $(12)_2$ and $V_l(r, r')$ the Green's kernel associated with the gravity potential, solution of $\mathscr{D}_l[V_l(r, r')] = -\delta(r - r')$ with $V_l(r, r') = V_l(\infty, r') = 0$, given by:

$$\frac{r'}{2l+1}\left(\frac{r}{r'}\right)^l \qquad \text{if } r \leqslant r'$$

$$\frac{r'}{2l+1}\left(\frac{r}{r'}\right)^{-l-1} \qquad \text{if } r \geqslant r',$$

and λ a non-dimensionalized number such that:

$$\lambda = \frac{4\pi G\rho_m R_1}{g_0} = \frac{3\,\rho_m}{(\rho_c - \rho_m)(R_c/R_1)^3 + \rho_m}.$$

Similarly:

$$H_I(r') = H_I^*(r') + \lambda\Delta\rho_I \left[\frac{H_I r_I^l + H_I r_I + H_c(r_c/r_I)^{l+1} r_c}{2l+1} - \alpha\rho(r')\, V_l(r_I, r')\right]. \tag{B2}$$

$$H_c(r') = H_c(r') + \lambda \Delta\rho_c \left[\frac{H_1 r_c^l + H_I (r_c/r_I)^l r_I + H_c r_c}{2l+1} - \alpha\rho(r')\, V_l(r_c, r') \right] . \qquad \text{(B3)}$$

For each r', the solution of the system (B1), (B2), (B3) allows us to get the value of the three kernels. Adopted values of non-dimensional $\Delta\rho_l$, $\Delta\rho_I$, $\Delta\rho_c$ are 1, 0, $(\rho_c - \rho_m)/\rho_m$ respectively. The contrast of density between the upper and lower mantle has been considered a negligible amount.